

Feasibility Simulation Analysis of Close-Proximity Construction of Underground Maglev Deep Foundation Pits Under Construction

Jingcheng Chen^{1,*}^a, Yiwen Yang¹, Bo Zeng², Bin Xie², Siwei Liu¹, Zhen Zhang³ and Yang Zhong⁴

¹China Construction Fifth Engineering Bureau Co., Ltd., Changsha 410004, Hunan, China

²China Construction Fifth Engineering Bureau Third Construction Co., Ltd., Changsha 410114, Hunan, China

³Hunan Sixth Engineering Co., Ltd., Changsha 410015, Hunan, China

⁴Hunan Airport Management Group Co., Ltd., Changsha 410100, Hunan, China

Keywords: Geotechnical Engineering, Numerical Analysis, Deep Foundation Pit, Close-Proximity Construction.


Abstract: To ensure the safety of deep excavations, construction is typically not allowed within a one-depth range around the excavation. In the Changsha Airport Comprehensive Transportation Hub project, the proposed West Parking Building is adjacent to an ongoing deep excavation for maglev construction, imposing constraints. To optimize the schedule, a construction plan was devised for the West Parking Building near the maglev deep excavation. Finite element analysis was employed to simulate the maglev deep excavation, assessing displacements and mechanical changes in the soil and support structures under different scenarios. The feasibility of the proximity construction plan was predicted, safety measures were proposed, and on-site implementation validated the analysis accuracy. Results indicate that, under favorable geological conditions, robust excavation support measures, and an appropriate proximity distance, the impact of proximity construction on deep excavations is minimal, rendering the plan feasible. This research provides valuable guidance for deep excavation construction.

1 INTRODUCTION

In recent years, the acceleration of urbanization and advancements in construction engineering have led to larger and more complex projects (Ming 2023). For example, these projects face complex and variable changes, such as groundwater levels and heterogeneity of soil (Vasilkin 2018). While existing research often qualitatively analyzes specific issues, there is a lack of systematic, dynamic analysis of the entire construction process (Gao X et al. 2023). Against this backdrop, ensuring the safety, efficiency, and economic viability of construction plans has become a pressing challenge in the field of geotechnical engineering.

Feasibility analysis of project plans is a crucial step in ensuring the efficient and safe completion of projects. Consequently, numerous scholars have conducted research in this area (AI T, 2021; Zhan et al. 2021). For instance, Yu Chunhong et al (Yu et al. 2019). conducted a feasibility analysis of foundation pit design schemes using anchor systems instead of steel

supports through theoretical calculations, addressing the difficulties and extended timelines associated with onsite steel support construction. Ma Linwei et al (Ma et al. 2022). conducted research on the feasibility of cross regional hydrogen water reverse transportation system engineering based on the approach of "scheme design and physical modeling → economic modeling of single agent operation mode → analysis of multi agent operation mode"; Cui Guoyong et al (Cui et al. 2022). quantitatively evaluated the feasibility of the new plan by analyzing the advantages and disadvantages of using TBM+main tunnel blasting method in terms of construction period and cost through construction organization design, including the plan of connecting the horizontal guide, construction inclined shaft, ventilation inclined shaft, and horizontal guide. Scholars have extensively researched various projects, employing different methods for feasibility analysis (Chen et al. 2020; Hua et al. 2020). However, there is scarce literature on the feasibility analysis of

^a <https://orcid.org/0009-0001-1432-3850>

magnetic levitation deep foundation pit construction using geotechnical engineering simulation software.

This paper uses geotechnical engineering numerical analysis software to simulate and analyze the feasibility of deployment plans for close-proximity construction. The safety of optimized schemes is validated through onsite implementation. The goal is to uncover the significant potential of geotechnical engineering numerical analysis in large construction projects and provide insights for improving construction management practices.

2 PROJECT STATUS

The Changsha Airport expansion project involves a comprehensive transportation hub spanning 492,300 square meters. It comprises an underground facility with four levels and five tracks, an aboveground interchange hub, and associated municipal facilities (see Figure 1). The complex network of deep foundation pits (see Figure 2) features interconnected excavations with varying elevations and shapes. Ensuring safety and efficiency during the construction phase of these foundation pits is pivotal to the overall success of the project.

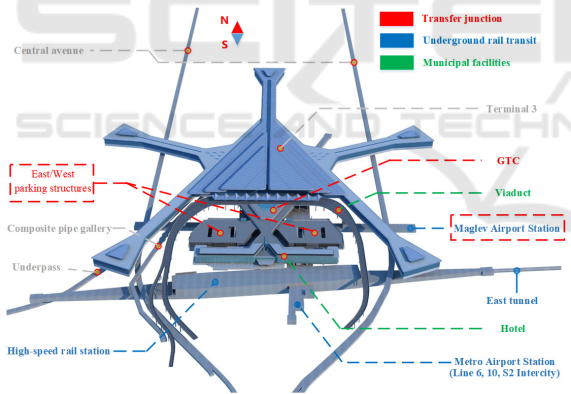


Figure 1: BIM model of structure.

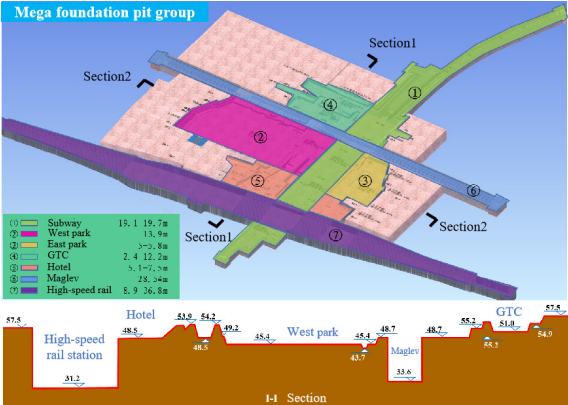


Figure 2: BIM model of deep foundation pit group.

Due to safety concerns, the original plan requires excavating the West Parking Building pit before moving on to the magnetic levitation pit. This sequence, waiting for the completion of the magnetic levitation structure, significantly impacts the West Parking Building construction schedule, posing considerable timeline risks. Urgent optimization of the West Parking Building pit design or adjustments to the construction plan are needed to alleviate schedule pressures (Figure 3).

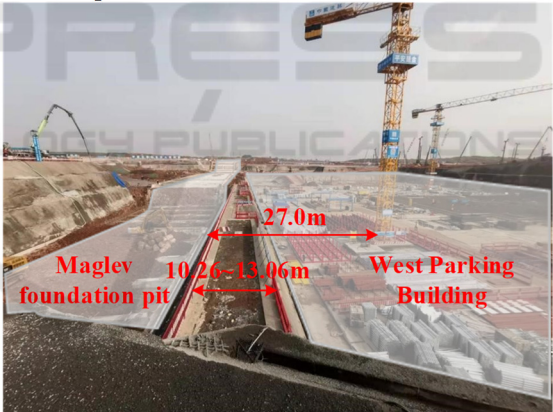


Figure 3: Status of the construction site.

3 PLAN OF CLOSE-PROXIMITY CONSTRUCTION

Given that both the magnetic levitation deep pit and the West Parking Building are in moderately weathered silty sandstone formations, and the West Parking Building is situated beyond the rupture plane of the magnetic levitation deep pit ($45^{\circ}+\varphi/2 = 60^{\circ}$), an expedited construction proposal has been introduced. The optimized plan suggests commencing the construction of the West Parking

Building structure in close proximity immediately after completing the internal support structure construction of the magnetic levitation deep pit. Due to construction coordination uncertainties, the most challenging scenario for this plan might occur when the magnetic levitation deep pit is excavated to its bottom while the West Parking Building reaches its peak load (maximum load), as depicted in Figure 4.

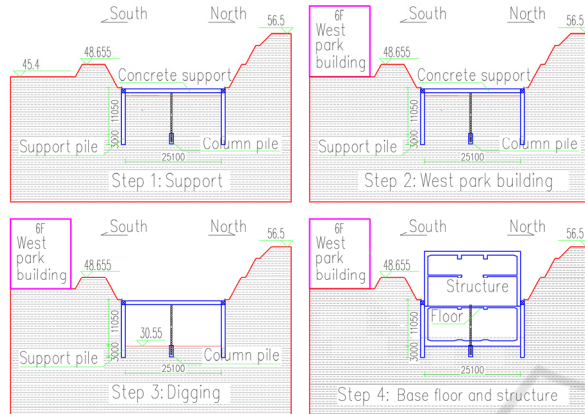


Figure 4: Condition of section 33 of the west parking building and maglev foundation pit of the original construction scheme.

To ensure the safe and stable implementation of the close-proximity construction plan for both the magnetic levitation deep pit and the West Parking Building, this study employs the finite element method to conduct numerical simulations, quantitatively analyzing the feasibility of the proposed scheme.

4 NUMERICAL SIMULATION AND RESULT ANALYSIS

4.1 Numerical Simulation Scheme

Using geotechnical finite element software, a 3D numerical model was created to simulate and analyze the safety of the magnetic levitation deep pit under two scenarios: the original design and the close-proximity construction plan. The aim is to assess the feasibility of the close-proximity construction plan. A 3D finite element geometric model was established for the adjacent area between the magnetic levitation deep pit and the West Parking Building based on construction drawings (see Figure 5).

In this area, the West Parking Building is divided into West 21 Zone (light green), West 22 Zone (dark green), and West 23 Zone (purple) moving from west to east, close to the magnetic levitation deep pit. The yellow marked area far from the magnetic levitation deep pit is designated as West 1 Zone.

The analysis involves studying ground displacement, deformation, stress distribution, and internal forces in the surrounding structures under both scenarios. Results will be compared with design specifications to assess the impact of the West Parking Building's close-proximity construction on the safety of the magnetic levitation deep pit. The construction plan considers the most adverse conditions and is reasonably simplified, as outlined in Table 1.

Table 1: Construction condition table.

Condition 1. The initial plan	Condition 2. Close-proximity construction plan
<p>Initial Stage: West Parking Building pit excavated to design elevation; magnetic levitation deep pit excavated to the bottom elevation of the crown beam, with installed retaining piles, column piles, grid columns, crown beams, and the initial concrete support.</p> <p>Step 1: Construction of a 6level structure in West 1 Zone, considering a 100 kPa load.</p> <p>Step 2: Excavation of the magnetic levitation deep pit to the bottom of the second support, with installation of steel supports, steel girders, and connecting beams.</p> <p>Step 3: Excavation of the magnetic levitation deep pit to the bottom elevation without constructing the base slab.</p>	<p>Initial Stage: Same as Scheme 1 "Initial Stage."</p> <p>Step 1: Same as Scheme 1 "Step 1."</p> <p>Step 2: Construction of the structure in West 2 Zone, with West 21 and West 22 completing 6 levels considering a load of 100 kPa; West 23 Zone remains unconstructed, serving as a temporary material storage area with a temporary load of 20 kPa considered for the most adverse conditions.</p> <p>Step 3: Same as Scheme 1 "Step 2."</p> <p>Step 4: Same as Scheme 1 "Step 3."</p>

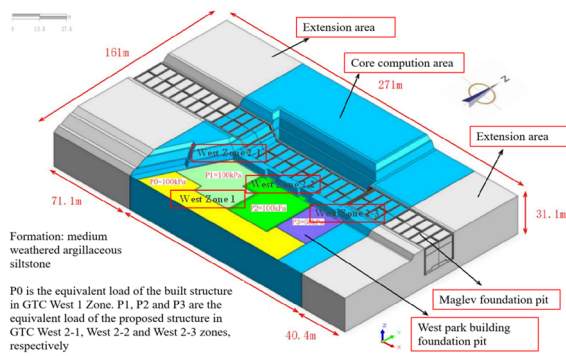


Figure 5: Formation geometry model.

4.2 Constitutive Model and Parameter Selection

The Mohr-Coulomb constitutive model is revised to a combined model with a power law relationship,

Table 2: Material parameter value table of numerical model.

Unit	Material	$\gamma(\text{kN}/\text{m}^3)$	μ	E(MPa)
Crown beam/Concrete support/Concrete tie bea	C30	25	0.20	30000
Column pile	C35	25	0.20	31500
Retaining pile	C35(reduction)	25	0.20	13230
Grid column/Steel connecting beam	Q235B	78	0.25	206000

The final established model core zone comprises 23 computational grid groups, 363, 106 elements, and 69, 569 nodes. The lateral and bottom boundary conditions are set as hinge supports and vertical displacement constraints, respectively. The West Parking Building structure is simplified based on zoning, and uniformly distributed surface loads are applied at corresponding positions in the model. Figure 6 illustrates a detailed view of the calculation model for the T3 station magnetic levitation pit.

comprising both a nonlinear elastic model and an elastoplastic model. Due to its capability to synchronize the elastic modulus during loading or unloading, it is suitable for numerical simulation studies of excavation in foundation pits. Therefore, the soil layer in the computational model is represented by an isotropic modified Mohr-Coulomb model. Constitutive models for structures such as crown beams, retaining piles, concrete supports, and grid columns utilize isotropic linear elastic models.

For moderately weathered silty sandstone, the values for density, cohesive strength, friction angle, and Poisson's ratio are 23.6 kN/m³, 80 kPa, 30°, and 0.25, respectively. The elastic, secant, tangent, and unloading moduli are 250 MPa, 321 MPa, 321 MPa, and 1607 MPa, respectively. For other material parameters, refer to Table 2 below.

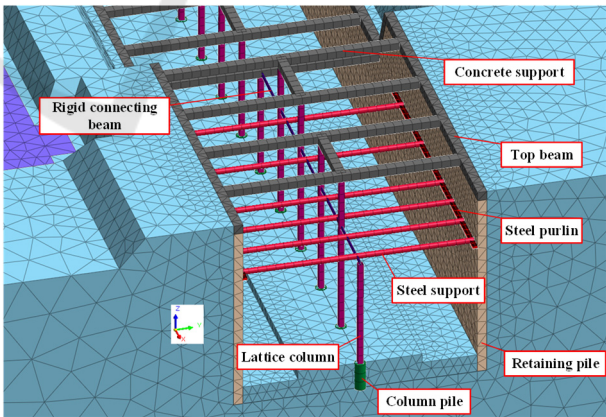


Figure 6: Details of foundation pit calculation model of Maglev T3 station.

4.3 Calculation Results and Analysis

Figure 7 illustrates vertical displacement contour maps of the ground and support structures under Conditions 1 and 2. After the excavation of the soil in

the magnetic levitation deep pit, the bottom soil experiences a certain degree of rebound due to the removal of soil loads, while the surrounding soil layers of the West Parking Building pit undergo settlement under the combined effects of construction loads and soil deformation. A comparison between Conditions 1 and 2 reveals that the impact of close-proximity construction on the rebound of the bottom soil in the magnetic levitation deep pit is minimal. However, it significantly affects the ground settlement in West 2 Zone, leading to a slightly increased settlement of the soil on the south side of the magnetic levitation deep pit. This shift changes the focus of settlement from the north side to the south side in the vicinity of the magnetic levitation deep pit.

Figure 8 shows the horizontal displacement contour maps of the ground and support structures under Conditions 1 and 2. After the excavation of the magnetic levitation deep pit, the horizontal displacement of the surrounding ground in the Y direction (north-south) primarily involves the inward movement of the soil on both sides of the pit. The maximum deformation is concentrated in the middle lower part of the retaining piles, with relatively larger values occurring at locations where there are significant changes in pit elevation. Comparing Conditions 1 and 2, close-proximity construction increases the horizontal displacement of the ground toward the interior of the magnetic levitation deep pit, with minimal impact on the form and characteristics of the ground's horizontal displacement.

Figure 9 presents the deformation contour map of the retaining piles under Conditions 1 and 2 (enlarged 1500 times to highlight deformation characteristics). Under the combined action of soil and water pressure, the retaining piles deform inward towards the magnetic levitation deep pit, with the maximum deformation concentrated in the middle lower part (specifically, 68m above the bottom of the pit). Comparing Conditions 1 and 2, close-proximity construction shifts the entire southside retaining pile parallel to the north side while increasing the deformation differences between different parts. However, the load from West 2 Zone has a relatively small impact on the deformation of the northside retaining pile.

Figure 10 displays the bending moment contour map of the retaining piles under Conditions 1 and 2. The maximum bending moments for the retaining piles on the north and south sides of the magnetic levitation deep pit occur at the bottom of the pit. Comparing Conditions 1 and 2, close-proximity construction mainly increases the maximum bending

moments of the retaining piles, with a greater increase on the south side.

Figure 11 illustrates the axial force contour map of the internal supports under Conditions 1 and 2. After the excavation of the magnetic levitation deep pit, both the concrete and steel support experience axial pressure, with the 112 axis of the concrete support receiving a higher axial pressure than other locations. Comparing Conditions 1 and 2, close-proximity construction increases the axial pressure on both the concrete and steel supports.

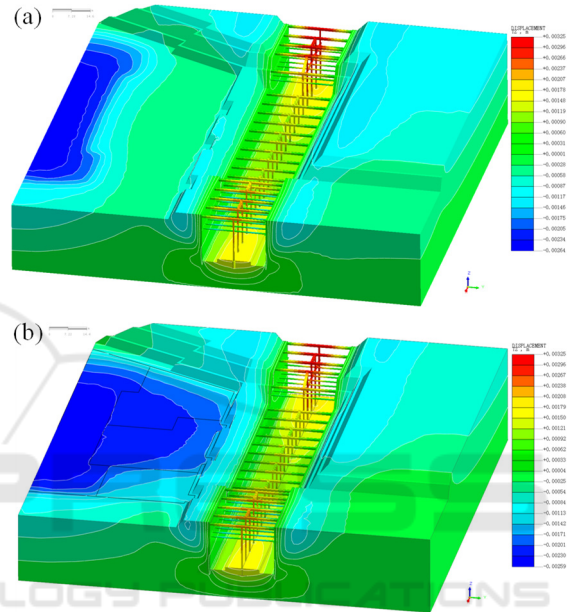
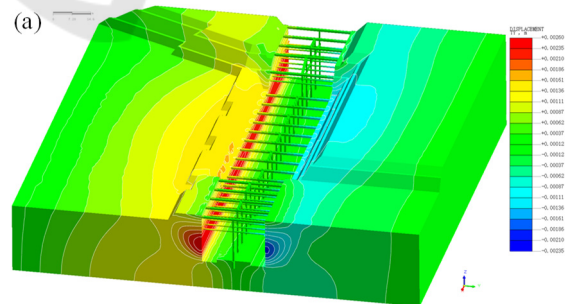


Figure 7: Vertical displacement cloud map of stratum and supporting structure under different working conditions (a) Operating condition 1; (b) Operating condition 2.



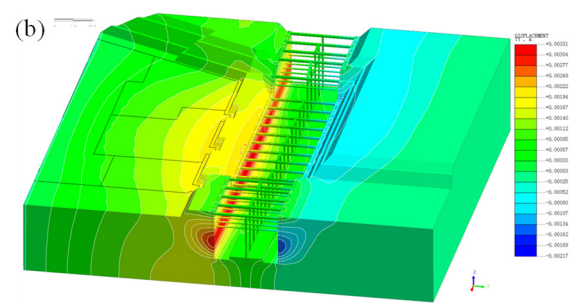


Figure 8: Horizontal displacement cloud map of stratum and support structure under different working conditions (a) Operating condition 1; (b) Operating condition 2.

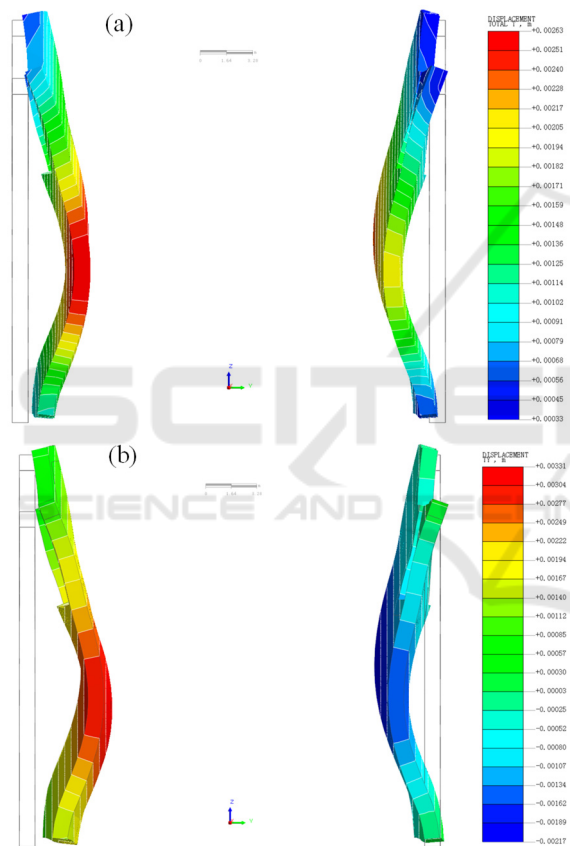


Figure 9: Deformation cloud map of envelope pile under different working conditions (1500 times larger than actual deformation) (a) Operating condition 1; (b) Operating condition 2.

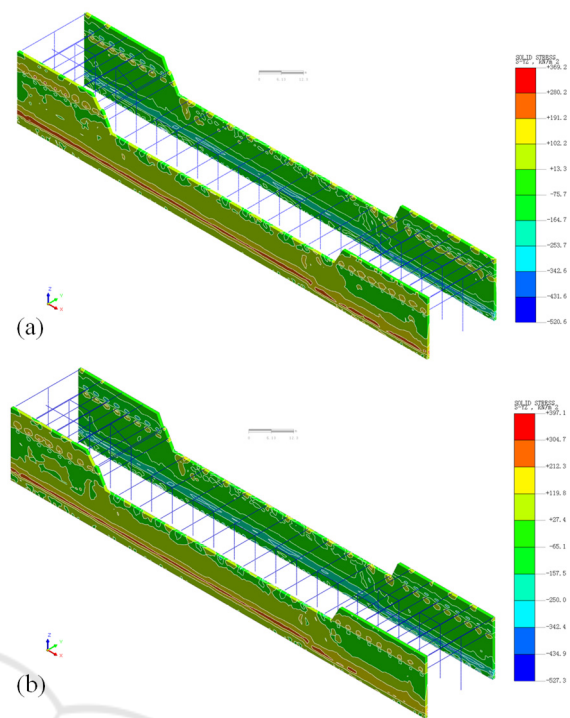


Figure 10: Cloud image of bending moment of retaining pile under different working conditions (a) Operating condition 1; (b) Operating condition 2.

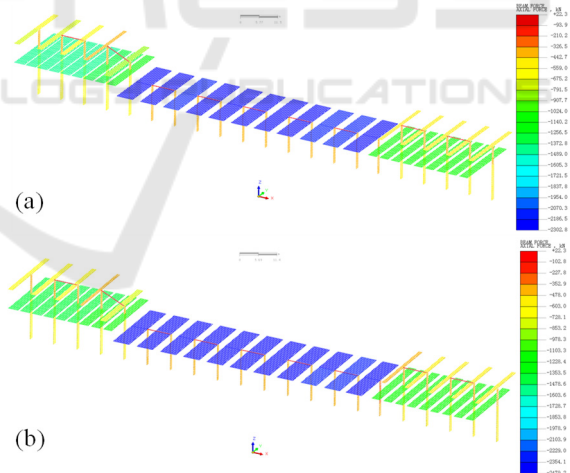


Figure 11: Axial force cloud diagram of internal support (concrete support, steel support) under different working conditions (a) Operating condition 1; (b) Operating condition 2.

Quantitative analysis was performed on the computed results extracted from different axial regions of the magnetic levitation deep pit under various conditions, comparing displacements with the original design requirements as shown in Figure 12. From Figure 12, it is observed that after applying the

West Parking Building load (Condition 2), the maximum horizontal, vertical, and deepseated displacements of the retaining pile head, as well as the maximum settlement of the surrounding ground, are all within the original design requirements. The safety calculations for various indicators in the optimized deployment plan have passed, and the displacement increments in Condition 2 relative to Condition 1 are relatively small. In summary, under the current conditions, directly constructing the West Parking Building (with varying construction levels in different zones) does not compromise the structural safety of the magnetic levitation deep pit.

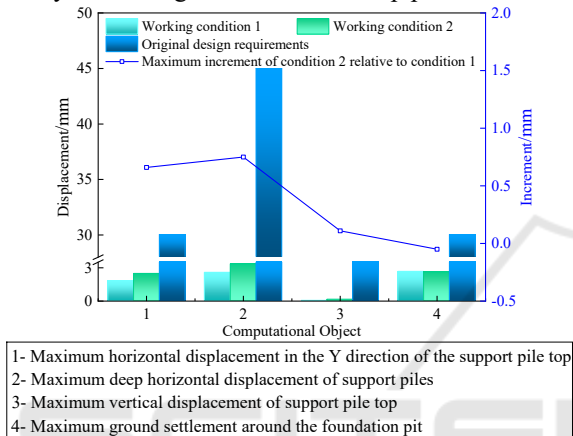


Figure 12: Comparison of displacement between different axis areas and original design requirements.

4.4 Construction Proposal

Although the simulation analysis indicates that the use of the close-proximity construction approach has minimal impact on the structural integrity of the magnetic levitation deep pit, it is imperative to implement appropriate safety measures to ensure the project's safety:

- (1) Strengthen pit monitoring: Enhance surface inspections, particularly during the rainy season, with a focus on crack observations; Timely collect and compile monitoring data. Report any alarming values promptly to relevant authorities for immediate action.
- (2) Ensure geological verification: Report any

inconsistencies with survey information promptly to ensure comprehensive information management throughout the project.

- (3) Develop emergency response plans: Equip emergency personnel, tools, and materials; Develop contingency plans for scenarios such as bottom pressure reversal and the need for additional anchors or steel supports.
- (4) Minimize loadings at intersections: Strictly prohibit overloading and excessive stacking phenomena, especially in areas designated for ridesharing vehicles and social buses.
- (5) Provide risk alerts: In case of a sudden increase in loads during actual construction, immediately cease operations and notify relevant authorities for reassessment.

5 RESULT OF FIELD IMPLEMENTATION

In February 2022, prior to onsite construction following the optimized deployment plan, displacement, stress, and water level monitoring sensors were installed in the magnetic levitation deep pit. Data were collected at daily intervals. To validate the applicability of numerical analysis in construction deployment optimization, monitoring data from the adjacent section of the magnetic levitation deep pit and West Parking Building were compared with numerical simulation results. Due to space limitations, the analysis focuses on the monitoring data of the settlement point with the highest average relative error with numerical simulation results (identified as CFDB0352). The layout of the settlement monitoring points is illustrated in Figure 13.

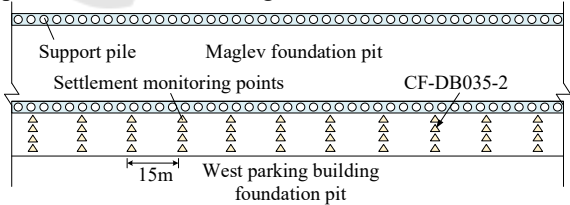


Figure 13: Schematic diagram of settlement monitoring point layout.

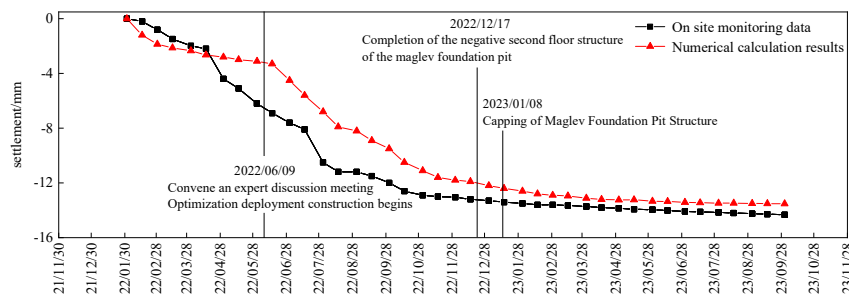


Figure 14: Comparison between onsite monitoring data and numerical simulation results of settlement monitoring points.

Figure 14 depicts the comparison curve between the actual measured data and numerical simulation results for the monitoring point labeled CFDB0352. As shown in the onsite monitoring data in Figure 14, the settlement value at the monitoring point continuously increased after the optimized deployment construction began, stabilizing after the completion of the magnetic levitation deep pit's negative second floor structure. The average relative error between the numerical simulation results and onsite monitoring data is 11.69%. The numerical simulation results are slightly lower than the onsite monitoring data, attributed to insufficient consideration of factors such as upper running vehicles and backfill loads during the numerical simulation.

6 CONCLUSION

This study employs dynamic management thinking and finite element analysis to simulate the feasibility of a proximity construction plan for an in-progress underground maglev deep excavation. The on-site implementation validates the safety of the plan. Results indicate that, under favorable geological conditions, robust excavation support measures, and an appropriate proximity distance, the construction near the maglev deep excavation poses no threat to structural safety. This application case effectively avoids the "nesting" phenomenon, offering valuable insights for similar construction feasibility analyses.

REFERENCES

Ming H. 2023. Strategies and Techniques of Life Cycle-Embodied Carbon Reduction from the Building and Construction Sector: A Review. *Journal of Architectural Engineering*, 29(3).

- Vasilkin A. 2018. Possibilities of applying structural optimization in building structures computer-aided design systems. *MATEC Web of Conferences*, 251, 03-017.
- Gao X, Xu X, Chen Q, et al. 2023. Research on Multi-objective Optimization Design Method of LID Facility Layout Scheme in Cold Land City. *Journal of Research in Science and Engineering*, 5(9).
- A I T, V A G. 2021. Increasing the economic efficiency of design and construction solutions due to the automated identification of construction works and structural elements of information models. *IOP Conference Series: Materials Science and Engineering*, 1083(1): 012-076.
- Zhan S, Qi L, Yu Z, et al. 2021. Analysis on the Influence of Shaft and Cross Passage Turn to the Main Line of Ingate under Different Construction Schemes. *Advances in Civil Engineering*, 2021.
- Yu C, Meng Z, Lu J, et al. 2019. Feasibility analysis and research on replacing steel support with deep foundation pit anchor system. *Construction Technology*, 48(S1): 201-3.
- Ma L, Han C, Li Z, et al. 2022. Design and Feasibility Analysis of Hydrogen Water Reverse Transportation System Engineering. *Journal of Power Engineering*, 42(11): 1024-32.
- Cui G, Huang Y, Chang Z, et al. 2022. Feasibility analysis of TBM application in the construction of the Yajiangeng tunnel's horizontal guide. *Construction Technology (Chinese and English)*, 51(02): 102-105.
- Chen Y, Wang H, Lv T, et al. 2020. Application of BIM Technology in the Construction Phase of Changsha Wanjiali Power Shield Tunnel Project [C]//Civil Engineering Graphics Branch of the China Graphics Society. 7th International BIM Technology Exchange Conference-Collection of Papers on Intelligent Construction and Innovative Development of Building Industrialization. China Construction Fifth Bureau Civil Engineering Co., Ltd.
- Hua K, Guo H, Li K, et al. 2020. Optimized Selection of Construction Scheme for Huiqing Expressway Tunnel. *IOP Conference Series: Materials Science and Engineering*, 741012092.